International Journal of Concrete Structures and Materials
Vol.1, No.1, pp.63~73, December 2007

Shear Capacity of Reinforced Concrete Beams Using Neural Network

Keun-Hyeok Yang[1)]*, Ashraf F. Ashour[2)], and Jin-Kyu Song[3)]

(Received May 7, 2007, Accepted November 5, 2007)

Abstract: Optimum multi-layered feed-forward neural network (NN) models using a resilient back-propagation algorithm and early stopping technique are built to predict the shear capacity of reinforced concrete deep and slender beams. The input layer neurons represent geometrical and material properties of reinforced concrete beams and the output layer produces the beam shear capacity. Training, validation and testing of the developed neural network have been achieved using 50%, 25%, and 25%, respectively, of a comprehensive database compiled from 631 deep and 549 slender beam specimens. The predictions obtained from the developed neural network models are in much better agreement with test results than those determined from shear provisions of different codes, such as KBCS, ACI 318-05, and EC2. The mean and standard deviation of the ratio between predicted using the neural network models and measured shear capacities are 1.02 and 0.18, respectively, for deep beams, and 1.04 and 0.17, respectively, for slender beams. In addition, the influence of different parameters on the shear capacity of reinforced concrete beams predicted by the developed neural network shows consistent agreement with those experimentally observed.

Keywords: neural network, deep beams, slender beams, shear capacity, code provisions

1. Introduction

Reinforced concrete beams are commonly classified as deep and slender beams according to their shear span-to-depth ratio.[1] Deep beams behave differently from shallow beams. Deep beams were identified as discontinuity regions where the strain distribution is significantly nonlinear and specific strut-and-tie models need to be developed, whereas shallow beams are characterised by linear strain distribution and most of the applied load is transferred through a fairly uniform diagonal compression field.

Based on many experimental and analytical studies,[2-5] the mechanisms of shear transfer in a cracked concrete slender beams include the shear in the uncracked concrete compression zone, aggregate interlock in diagonal crack planes, dowel action of longitudinal reinforcement, and truss action of vertical web reinforcement. On the other hand, deep beams, having a nonlinear strain distribution over the cross-section depth due to a smaller shear span-to-overall depth ratio and extraordinarily high concentric load, carry a significant amount of the applied load by strut-and-tie action. Owing to shear deformation and redistribution of stresses in cracked concrete struts, the conventional beam theory or shear hypotheses developed for slender beams would not be applicable to deep beams.

[1)]KCI member, Dept. of Architectural Engineering, Mokpo National University, Mokpo 534-729, Korea. *E-mail: yangkh@mokpo.ac.kr*
[2)]EDT1, School of Engineering, Design and Technology, University of Bradford, Bradford, BD7 1DP, UK.
[3)]KCI member, Dept. of Architectural Engineering, Chonnam National University, Gwangju 500-843, Korea.

The problem of shear in reinforced concrete has been extensively studied for about a century.[6] And yet, there is no agreed rational procedure to predict the shear strength of reinforced concrete beams. Reineck et al.[7] pointed out that most of the proposed models to evaluate shear capacity of slender beams would be inadequate for general acceptance as they were empirical and calibrated to fit limited shear test results. In addition, Yang and Ashour[8] showed that most code provisions for shear design of deep beam, such as ACI 318-99,[9] CIRIA Guide 2,[10] ACI 318-05[11] and EC 2,[12] generally fail to adequately capture the effect of different parameters on the shear capacity contributions of concrete and web reinforcement.

Artificial neural network (NN) techniques are generally known to be a useful tool to adequately predict structural behaviour of concrete members if many reliable test data are available.[3,13,14] Bohigas,[3] and Sanad and Saka[14] showed that shear strength of slender and deep beams, respectively, can be better predicted by multi-layered feed-forward NNs than other existing formulas. However, it should be noted that NNs are hardly capable of giving extrapolations for problems outside the network training set as they can learn and generalise through only previous patterns.[15] Therefore, it is important to train NNs with more reliable test data whenever they become available to produce acceptable solutions to different applications.

The present study develops multi-layered feed-forward NNs trained with the back-propagation algorithm to model the nonlinear relationship between shear capacities of both deep and slender beams and different influencing parameters. An extensive database for deep and slender beams tested by different researchers are compiled and used to train, generalize and verify the developed NNs. Statistical distributions of predictions obtained

from the trained NN are compared with those determined from shear provisions such as, ACI 318-05,[11] EC 2[12] and Korean Building Code - Structural (KBCS).[16] Also, a parametric study is carried out to ensure successful building, training and validation of the developed NNs.

2. Neural network modelling

2.1 Review of network architecture with back-propagation

A typical multi-layered feed-forward NN without input delay is composed of an input layer, one or more hidden layers and an output layer as shown in Fig. 1, where **P** indicates the input vector, **IW** and **LW** give the weight matrices for input and hidden layers, respectively, **b** represents the bias vector, and **n** is the net input passed to the transfer function ***f*** to produce the neuron's output vector ***y***. Input data in the input layer given from outside feed into the hidden layers connecting input and output layers in forward direction, and then useful characteristics of input data are extracted and remembered in the hidden layers to produce NN predictions through the output layer. Each processing unit can send out only one output although it would have various inputs. The outputs of each intermediate hidden layer turn to inputs to the following layer.

Among the available techniques to train a network, back-propagation is generally known to be the most powerful and widely used for NN applications[3, 14]. To get some desired outputs, weights, which represent connection strength between neurons, and biases are adjusted using a number of training inputs and the corresponding target values. The network error, difference between calculated and expected target patterns in a multi-layered feed-forward network, is then back propagated from the output layer to the input layer to update the network weights and biases. The adjusting process of neuron weights and biases is carried out until the network error arrives at a specific level of accuracy.

2.2 Generalization

One of the problems that occurs during NN training is the so called overfitting as the network has memorized the training features, but it has not learned to generalize new patterns.[15] Shi[18] showed that training data evenly distributed over the entire space enables the NN to successfully achieve the desired behaviour and produce a smaller network error for new input data. Early stopping technique is generally recognized to be one of the most effective methods to improve generalization of NNs.[15,17] In this technique, the available data are divided into three subsets; training, validation and test subsets. The training set is used for computing the gradient and updating the network weights and biases to diminish the training error. When the error on the validation set, which is monitored during the training process, increases for a specified number of iterations, the training is stopped, and then

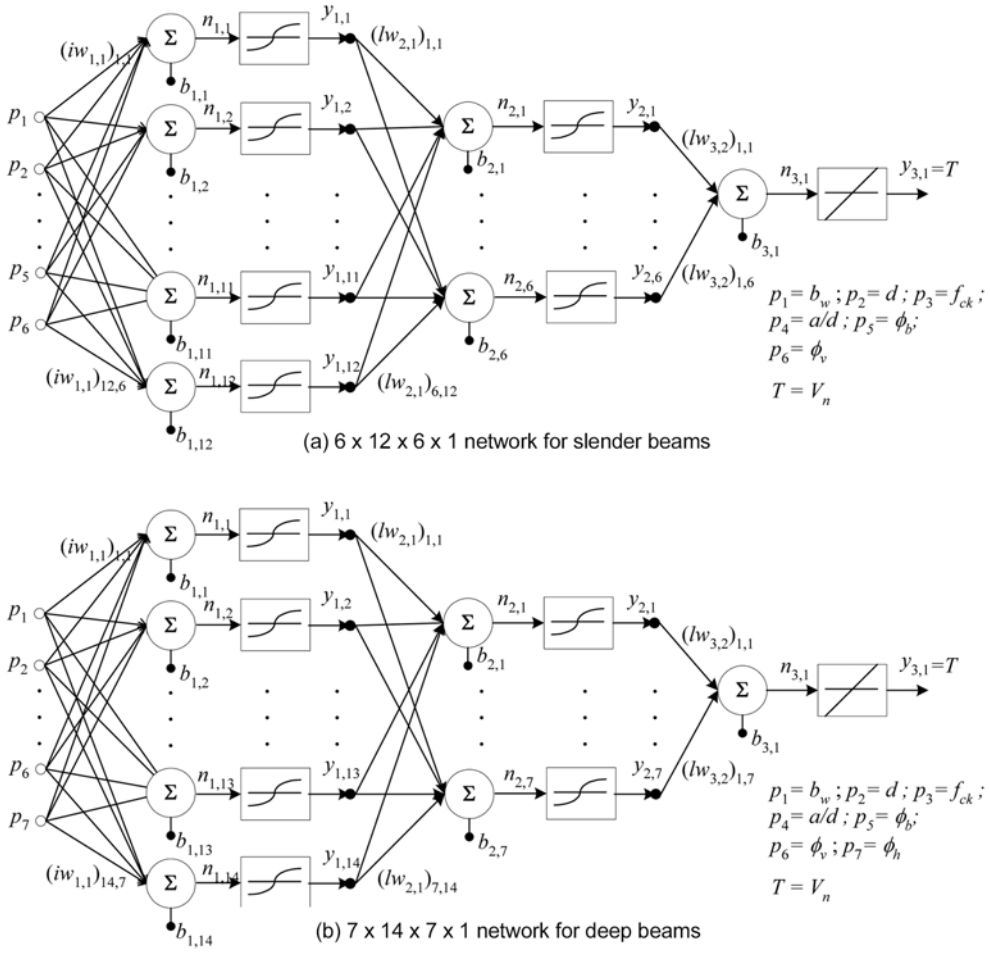

Fig. 1 Architecture of networks for reinforced concrete beams.

the network weights and biases at the minimum validation error are returned. The test set error is not used during the training, but it is used for verification of the NNs and comparison of different models.

2.3 Experimental database

A total of 1180 reinforced concrete beam specimens failed in shear are compiled from different sources including the database for deep beams established by Yang and Ashour,[8] existing slender beam details presented by Bohigas,[3] and beam data tested in Korea and Japan collected by Chung.[18] ACI 318-05 and EC 2 define beams having shear span-to-overall depth ratio a/h at less than 2.0 and clear shear span-to-overall depth ratio a_v/h not exceeding 2.0, respectively, as deep beams, where a = shear span, h = overall section depth, and a_v = clear shear span. When the overall beam depth h is not recorded in the database, beams having a/d below 2.2 ($\approx a/h \le 2.0$) were classified as deep beams in the database, where d = effective section depth. As a result, a total of 631 deep beams and 549 slender beams were identified to develop the two NNs shown in Fig. 1.

Some test specimens had no web reinforcement whereas others were reinforced with vertical or horizontal web reinforcement: the number of deep and slender beams in the database is 240 and 411, respectively, for beams without web reinforcement, 169 and 138, respectively, for beams with only vertical web reinforcement. In addition, the number of deep beams with horizontal and orthogonal web reinforcement is 59 and 163, respectively. The database ascertained that the shear capacity of both deep and slender beams was influenced by geometrical conditions such as section width, b_w, and effective section depth, d, longitudinal reinforcement ratio $\rho_b = A_s/b_w d$, vertical web reinforcement ratio $\rho_v = A_v/b_w s_v$, and shear span-to-effective depth ratio a/d, and material properties such as concrete compressive strength, f_{ck}, and yield strength, f_y, of reinforcement, where A_s = area of longitudinal reinforcement, A_v and S_v = area and spacing of vertical web reinforcement, respectively, as shown in Fig. 2. In addition, the shear capacity of deep beams would be also influenced by the horizontal web reinforcement ratio $\rho_h = A_h/b_w s_h$ as proved by Yang et al.[19] that the smaller a/d, the more effective the horizontal web reinforcement, where, A_h and s_h = area and spacing of horizontal web reinforcement, respectively. As the effect of web reinforcement on the shear capacity is commonly dependent on concrete strength, web reinforcement ratio was normalised with respect to concrete strength.

Six neurons representing the width, b_w, effective depth, d, concrete strength, f_{ck}, longitudinal reinforcement ratio, ρ_b, vertical web reinforcement index, $\phi_v = \dfrac{\rho_v f_{yv}}{f_{ck}}$ and shear span-to-effective depth ratio, a/d, were used in the input layer of the NN developed for the slender beams as shown in Fig. 1 (a), where f_{yv} = yield strength of vertical web reinforcement. Whereas a seventh neuron representing the horizontal web reinforcement index, $\phi_h = \dfrac{\rho_h f_{yh}}{f_{ck}}$, was added to the input layer of the developed NN for deep beams as shown in Fig. 1 (b), where f_{yh}= yield strength of horizontal web reinforcement. Shear capacity V_n at failed shear span was the only output of the NNs developed.

Table 1 gives the ranges of input data in training, validation and test subsets used to develop the NNs. In the database, beam width of deep and slender beams ranged from 20 to 300 mm and from 100 to 457 mm, respectively, effective section depth is between 80 and 1,559 mm for deep beams and between 110 and 1,090 mm for slender beams, and longitudinal reinforcement ratio ranged between 0.0011 and 0.066 for deep beams and between 0.0028 and 0.066 for slender beams. The maximum vertical web reinforcement indices for deep and slender beams were 0.964 and 0.14, respectively, and the maximum horizontal web reinforcement index for deep beams was 1.847. The test specimens were made of concrete having a very low compressive strength of 11.2 MPa and 14.7 MPa for deep and slender beams, respectively, and a high compressive strength of 120 MPa and 125 MPa for deep and slender beams, respectively. Training, validation and test subsets had 50%, 25%, and 25% of all specimens in the database, respectively. The input data in each subset were selected at equally spaced points throughout the database so that the range of input in training subset would cover the entire distribution of database and input in validation subset would stand for all points in training subset as shown in Table 1.

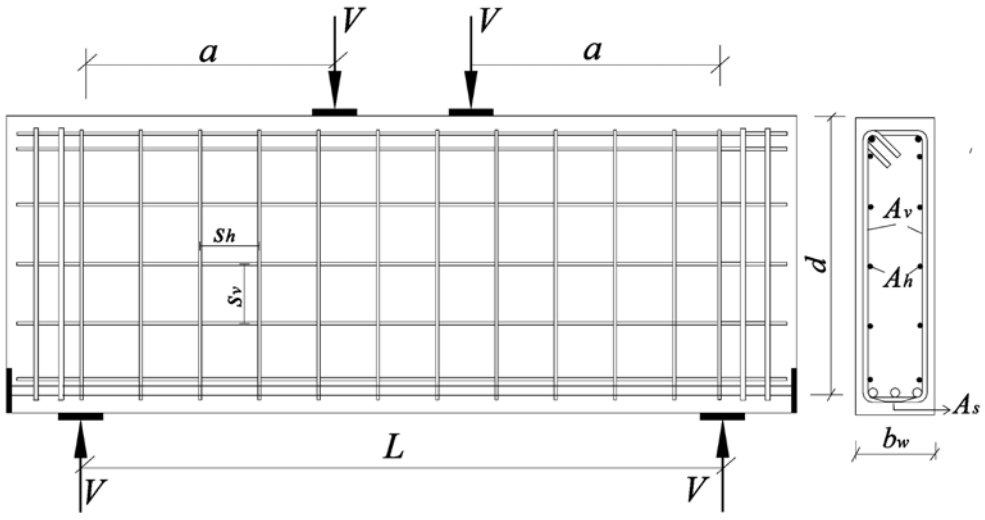

Fig. 2 Details of reinforced concrete beams in the database.

Table 1 Range of input data in the database used to generalize the developed NNs.

Input variables*		Total data		Training subset		Validation subset		Test subset	
		min	max	min	max	min	max	min	max
b_w (mm)	Deep beams	20	300	20	300	20	300	20	300
	Slender beams	100	457	100	457	100	457	100	457
d (mm)	Deep beams	80	1559	80	1559	135.5	1559	135.5	1559
	Slender beams	110	1090	110	1090	136	1090	136	1090
f_{ck} (MPa)	Deep beams	11.2	120	11.2	120	12.3	98.1	12.3	120
	Slender beams	14.7	125	14.7	125	16.3	103.2	16.7	125
a/d	Deep beams	0.24	2.2	0.24	2.2	0.24	2.2	0.24	2.2
	Slender beams	2.25	9.0	2.25	9.0	2.3	8.0	2.25	8
ρ_b	Deep beams	0.0011	0.066	0.0011	0.066	0.0012	0.058	0.0019	0.058
	Slender beams	0.0028	0.066	0.0028	0.066	0.0047	0.05	0.0047	0.066
ϕ_v	Deep beams	0.0	0.964	0.0	0.964	0.0	0.647	0.0	0.494
	Slender beams	0.0	0.14	0.0	0.14	0.0	0.129	0.0	0.14
ϕ_h	Deep beams	0.0	1.847	0.0	1.847	0.0	1.509	0.0	1.493

2.4 Building of neural network

The NN toolbox available in MATLAB version 6.0,[20] which can be conveniently implemented to model large-scale problems, was used for building of the current NN model. In a multi-layered NN having a back-propagation algorithm, the combination of nonlinear and linear transform functions can result in well trained process. In the present NNs, tan-sigmoid and linear transform functions were employed in the hidden and output layers, respectively. As upper and lower bounds of tan-sigmoid function output are +1 and -1, respectively, input and target in the database were normalized using Eq. (1) below so that they fall in the interval [-1, 1]. NNs can also have better efficiency with the normalization of original data.[15, 21]

$$(P_i)_n = \frac{2(p_i - (p)_{\min})}{(p)_{\max} - (p)_{\min}} - 1 \tag{1}$$

where (p_i) and p_i = normalized and original values of data set, and $(p)_{\min}$ and $(p)_{\max}$ = minimum and maximum values of the parameter under normalization, respectively. Also, after training and simulation, outputs having the same units as the original database can be obtained by rearranging Eq. (1) as follows

$$p_i = \frac{[(p_i)_n + 1][(p)_{\max} - (p)_{\min}]}{2} + (p)_{\min} \tag{2}$$

Overfittings and predictions in training and outputs of NNs are commonly influenced by the number of hidden layers and neurons in each hidden layer. Therefore, trial and error approach was carried out to choose an adequate number of hidden layers and number of neurons in each hidden layer as given in Table 2. In addition, NN performance is significantly dependent on initial conditions[15] such as initial weights and biases, back-propagation algorithms, and learning rate. In NNs presented in Table 2, the following features were applied when

- $a/d \leq 2.2$ in the input layer and all data for beam specimens related to NNs developed for deep beams, otherwise NNs developed for slender beam were employed.
- Initial weights and biases were randomly assigned by MATLAB version 6.0.
- Resilient back-propagation algorithm was used for back-propagation (a slower convergence was more effective in early stoppage to generalize NN[21]).
- The learning rate and momentum factor were 0.4 and 0.2, respectively.[14]
- Mean square error (MSE) was used to monitor the network

Table 2 Statistical comparison of outputs and targets in different network structures

Network structures*		Mean ($\gamma_{cs,m}$)	Standard deviation ($\gamma_{cs,s}$)	Coefficient of determination (R^2)
Deep beams	7×7×1	1.034	0.266	0.926
	7×14×1	1.028	0.252	0.939
	7×21×1	1.019	0.251	0.94
	7×14×7×1	1.033	0.227	0.942
	7×21×7×1	1.044	0.253	0.921
	7×14×7×7×1	1.042	0.229	0.931
Slender beams	6×6×1	1.045	0.219	0.905
	6×12×1	1.037	0.23	0.911
	6×18×1	1.036	0.222	0.923
	6×12×6×1	1.05	0.188	0.929
	6×18×6×1	1.076	0.24	0.897
	6×12×6×6×1	1.057	0.198	0.918

* The first and the last numbers indicate the numbers of neurons in input and output layers, respectively, and the others refer to the number of neurons in hidden layers.

performance, where MSE = $\frac{1}{N}\sum_{i=1}^{N}(T_i - A_i)^2$, N= total number of training set, T_i and A_i= target and actual output of specimen i, respectively.

- The maximum number of iterations (epochs) was 300.

The training process stopped when one of the following conditions was satisfied:

- the maximum number of epochs was reached;
- the performance was minimized to the required target;
- MSE was less than 0.0001;
- the performance gradient fell below a minimum value; or
- the validation set error started to rise for a number of iterations.

Statistical comparisons between outputs and targets for the total points of database for both deep and slender beams according to the number of hidden layers and the number of neurons in each hidden layer are given in Table 2. Each statistical value in Table 2 is an average calculated from 30 different trials, as different random initial weights and biases are employed in each trial. Although the mean and standard deviation of the ratio of predicted and measured shear capacities of beams presented in Table 2 by different NN architectures were close to each other, 7×14×7×1 and 6×12×6×1 networks were the most successful for deep and slender beams, respectively. Therefore, the 7×14×7×1 and 6×12×6×1 networks to predict shear capacity of deep and slender beams, respectively, were finally selected as presented in Fig. 1. The initial weights and biases achieved the highest coefficient of determination of all 30 trials were selected for the initial weights and biases of the ultimate $7 \times 14 \times 7 \times 1$ and 6×12×6×1 NNs.

3. Comparison with code provisions

3.1 Review of shear provisions in current codes of practice

Shear provisions specified in different codes, such as KBCS, ACI 318-05 and EC 2, are summarized in Table 3. Figure 3 also presents the load transfer mechanism by truss action of vertical web reinforcement in slender beams and strut-and-tie action in deep beams. KBCS provisions, using the empirical equations of ACI 318-99, assume that the shear capacity of both deep and slender beams as a combination of shear transfer capacities of concrete and web reinforcement as given in Eq. (3) are presented in Table 3. Shear transfer capacity of concrete is based on the diagonal cracking strength of slender beams tested without web reinforcement and the factor $\left(3.5 - 2.5\frac{M_u}{V_u d}\right)$ is employed to reflect the shear capacity enhancement due to arch action in deep beams. Shear transfer capacity of web reinforcement in slender and deep beams is evaluated from 45° truss model and empirical model proposed by Crist,[22] respectively, Eq. (7), referring to shear transfer capacity of web reinforcement in deep beams shows that a higher shear can be carried by horizontal web reinforcement than vertical web reinforcement when l_n/d is less than 5.0, regardless of a/d. However, several researchers[1,8,14,19] concluded that the empirical equations for shear capacity of deep beams specified in ACI 318-99 are unsuitable for considering strength enhancement due to strut action of concrete and reflecting relative effectiveness of horizontal and vertical web reinforcement against the variation of a/d.

In ACI 318-05, shear provisions for slender beams are the same as those of ACI 318-99, while shear design for deep beams using strut-and-tie models is specified. When the total web reinforcement ratio in two orthogonal directions in each face is more than 0.003, the effectiveness factor of concrete would be increased to 0.75 instead of 0.6, regardless of concrete strength and the amount of web reinforcement. This implies that the arrangement of web reinforcement satisfying the specified minimum web reinforcement allows the shear capacity of deep beams predicted by the strut-and-tie model to be increased by 25%. No provisions for shear transfer mechanism of web reinforcement in deep beams are provided.

EC 2 also specifies shear provisions for slender and deep beams using empirical equations and strut-and-tie models, respectively. The equations for slender beams without web reinforcement consider the influence of concrete strength, dowel action of longitudinal reinforcement and size effect, whereas neglect the effect of shear span-to-depth ratio as given by Eq. (10). Unlike Eq. 3 (see Table 3) used by KBCS and ACI318-05, EC2 requires that the shear capacity of slender beams requiring web reinforcement is determined from the shear transfer capacity of only web reinforcement ignoring the contribution of concrete. The shear transfer capacity of vertical web reinforcement is obtained from variable-angle truss model; however, the slope of diagonal cracking planes is limited between 21°($\cot\theta = 2.5$) and 45° ($\cot\theta = 1.0$). Therefore, shear capacity of slender beams with vertical web reinforcement can be predicted using Eq. (11). Strut-and-tie models for deep beams are very similar to those specified in ACI 318-05, except for the effectiveness factor of concrete, which is dependent on concrete compressive strength and does not consider the effect of web reinforcement.

3.2 Results and discussions of code comparisons

The effect of shear span-to-effective depth ratio a/d, which is one of the critical variables distinguishing between beam action and strut-and-tie action, on the normalized shear capacity $\lambda_n = \frac{V_n}{b_w d\sqrt{f_{ck}}}$ of beams without web reinforcement, is shown in Fig. 4. Geometrical dimensions and concrete strength adopted to obtain predictions by different codes are the average values of those of database beam specimens employed in Fig. 4; namely, b_w, d, f_{ck}, and ρ_b used in code predictions of Fig. 4 were 175 mm, 355 mm, 45 MPa, and 0.002, respectively. Test results showed that shear capacity of beams significantly increased with the decrease of a/d when a/d was below around 2.5, while that of beams having a/d larger than 2.5 exhibited less variation due to the change in a/d. Therefore, it can be concluded that the effect of a/d on the shear capacity of beams would be more important in deep beams than in slender beams. In addition, predictions obtained from different codes are more sensitive to a/d in deep beams rather than in slender beams. Shear capacity predicted from empirical formula of KBCS is highly conservative in beams having a/d below 1.0. In predictions by ACI 318-05 and EC 2, a discontinuous trend appears at the threshold a/d distinguishing deep and slender beams as shear capacities of deep and slender beams. This trend is evaluated using strut-and-tie models and

Table 3 Summary of shear provisions specified in different codes.

Code provisions	Shear capacity (V_n)	
KBCS	$V_n = V_c + V_s$	(3)
	For slender beams	
	$V_c = \left[0.16\sqrt{f_{ck}} + 17.6\rho_b \frac{V_u d}{M_u}\right] b_w d \le 0.29\sqrt{f_{ck}} b_w d$	(4)
	$V_s = \rho_v f_{yv} b_w d$	(5)
	For deep beams	
	$V_c = \alpha_d \left[0.16\sqrt{f_{ck}} + 17.6\rho_b \frac{V_u d}{M_u}\right] b_w d \le 0.5\sqrt{f_{ck}} b_w d$	(6)
	$V_s = \left[\rho_v f_{yv}\left(\frac{1 + l_n/d}{12}\right) + \rho_h f_{yh}\left(\frac{11 - l_n/d}{12}\right)\right] b_w d$	(7)
	$V_n \le \frac{2}{3}\sqrt{f_{ck}} b_w d \quad \text{for } l_n/d \le 2$ $\le \frac{1}{18}(10 + l_n/d)\sqrt{f_{ck}} b_w d \quad \text{for } 2 < l_n/d \le 5$	(8)
	where $\alpha_d = \left(3.5 - 2.5\frac{M_u}{V_u d}\right) \le 2.5$	
ACI 318-05	For slender beams V_n = same equations as those specified in KBCS	
	For deep beams $V_n = V_e f_{ck} b_w w_s \sin\theta_s$	(9)
	where $v_e = 0.75$ for beams having orthogonal web reinforcement ratio with $\sum \frac{A_{wj}}{b_w s_{wj}} \sin(\theta_r)_j \ge 0.003$ and otherwise 0.6; $\tan\theta_s = jd/a \ge 0.488$; $jd = h - (w_t \mid w_t')/2$; $w_t' = 1.25 w_t$; and $w_s = \frac{2.25 w_t \cos\theta_s + [(l_p)_E + (l_p)_p]\sin\theta_s}{2}$	
EC 2	For slender beams without web reinforcement	
	$V_n = V_c = \left[0.18 k_1 (100\rho_b f_{ck})^{\frac{1}{3}}\right] b_w d \ge 0.035 k_1^{1.5}\sqrt{f_{ck}} b_w d$	(10)
	where $k_1 = 1 + (200/d)^{0.5} \le 2$, $\rho_b \le 0.02$	
	For slender beams with web reinforcement	
	$V_n = Max[V_c, (\rho_v f_{yv}\cot\theta) bjd] \le v_e \frac{f_{ck}}{1.5}/(\cot\theta + \tan\theta)$	(11)
	where $v_e = 0.6(1 - f_{ck}/250)$, $j = 0.9$, $1 \le \cot\theta \le 2.5$	
	For deep beams $V_n = v_e f_{ck} b_w w_s \sin\theta_s$ where $w_t' = 1.176 w_t$, $w_s = \frac{2.176 w_t \cos\theta_s + [(l_p)_E + (l_p)_p]\sin\theta_s}{2}$	(12)

Note : Definitions of different parameters used in the above formulas are given in the list of notation section.

empirical section models based on test results. Shear capacity predicted from EC 2 is generally lower than that obtained from ACI 318-05, regardless of the variation of a/d.

Table 4 gives the mean and standard deviation of the ratio

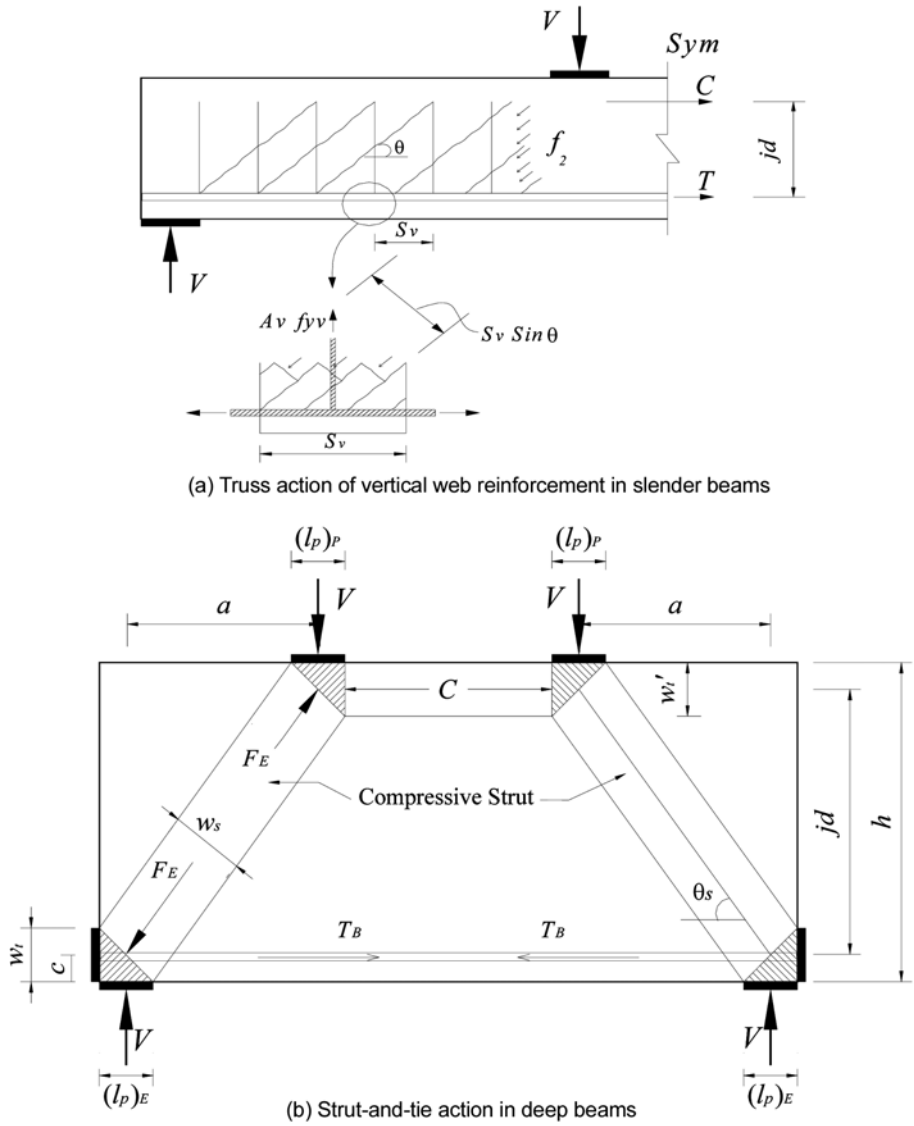

Fig. 3 Schematic load transfer mechanisms for reinforced concrete slender and deep beams.

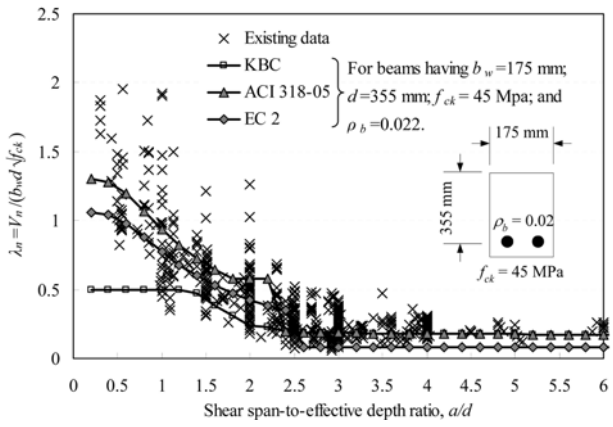

Fig. 4 Effect of a/d on λ_n of beams without web reinforcement.

between predicted and measured shear capacities, $\gamma_{cs} = (V_n)_{Pre.}/(V_n)_{Exp}$, of deep and slander beams with different web reinforcement arrangement. The distributions of γ_{cs} for beam specimens in the database against a/d are also shown in Fig. 5. For deep beams without web reinforcement, a higher conservatism is observed in KBCS's model than the other two code models. However, KBCS's model for deep beams with horizontal web reinforcement and slender beams having a/d less than 5.0 turns to be unconservative. It also overestimates shear transfer capacity of vertical web reinforcement by truss model in slender beams. The mean and standard deviation of γ_{cs} for slender beams obtained from ACI 318-05 are the same as those of KBCS because the same equation is employed in both code provisions. Strut-and-tie models specified in ACI 318-05 and EC 2 become highly unconservative with the increase of a/d and higher $\gamma_{cs,m}$ and $\gamma_{cs,s}$ are observed in deep beams without web reinforcement than in deep beams with web reinforcement as shown in Table 4 and Fig. 5. EC 2 provisions for slender beams are highly conservative for beams having a/d more than 4.0. However, shear transfer capacity of vertical web reinforcement in slender beams predicted from EC 2 using the slope of diagonal cracking planes of 21° ($\cot\theta = 2.5$) is unconservative as shown in Fig. 5 (c). On the other hand, predictions obtained from the developed NNs are in better agreement with test results regardless of shear span-to-overall depth ratio and configuration of web reinforcement; $\gamma_{cs,m}$ and $\gamma_{cs,s}$ are 1.02 and 0.18, respectively, for deep beams, and 1.04 and 0.17, respectively, for slender beams.

Table 4 Statistical comparisons of predictions by different methods.

Statistical values	Beam	Models		W/O	W/V	W/H	W/VH	Total
$\gamma_{cs,\,m}$	Deep	Neural network		1.05	1.0	1.02	1.01	1.02
		KBCS		0.6	0.58	0.78	0.7	0.64
		ACI 318-05		1.36	0.85	0.79	1.0	1.08
		EC 2		1.05	0.67	0.64	0.66	0.81
	Slender	Neural network		1.05	1.0	-		1.04
		KBC (ACI 318-05)		0.84	0.84			0.84
		EC 2	cot θ=1	0.62	0.5			0.59
			cot θ=2.5		0.8			0.67
$\gamma_{cs,\,s}$	Deep	Neural network		0.2	0.17	0.16	0.14	0.18
		KBCS		0.21	0.19	0.27	0.17	0.21
		ACI 318-05		0.82	0.37	0.35	0.33	0.62
		EC 2		0.54	0.26	0.22	0.18	0.42
	Slender	Neural network		0.18	0.13	-		0.17
		KBCS&ACI 318-05		0.32	0.26			0.3
		EC 2	cot θ=1	0.47	0.32			0.44
			cot θ=2.5		0.34			0.45

Note : $\gamma_{cs,\,m}$ and $\gamma_{cs,\,s}$ indicate the mean and standard deviation for the factor γ_{cs}, respectively.
W/O, W/V, W/H, and W/VH refer to beams without, with only vertical, with only horizontal and with orthogonal web reinforcement, respectively.

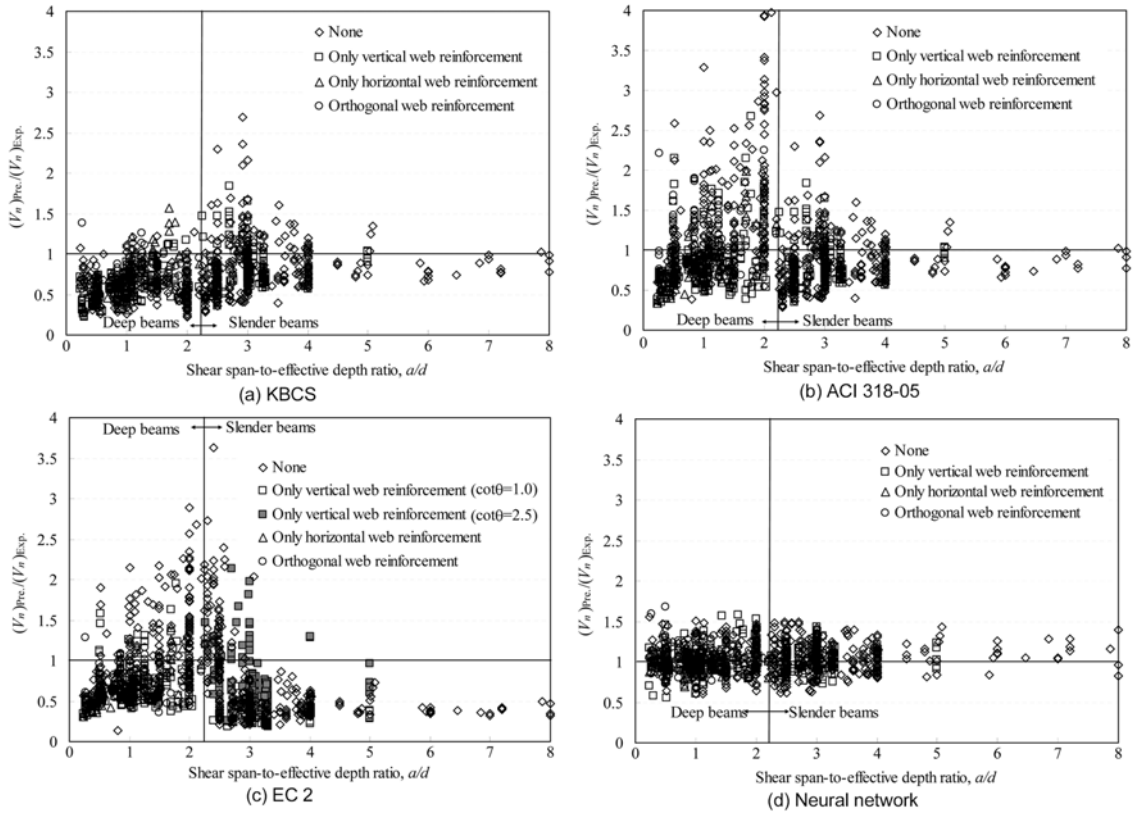

Fig. 5 Comparisons of predicted and measured shear capacities in different models.

4. Parametric analysis

The influence of main parameters on the shear capacity of reinforced concrete beams is studied using the developed NNs and experimental results in the database. The results predicted from this parametric study can also ensure whether training and validation subsets in the developed NN were successfully built. In Fig. 6 to Fig. 8, white symbols and curves with black symbols indicate the experimental results in the database and predictions obtained from the developed NNs, respectively. As the shear capacity of reinforced concrete beams commonly increases in proportion to the square root of concrete strength,[1,2,11] experimental results and predictions in this parametric study are accordingly normalized as $\frac{V_n}{b_w d\sqrt{f_{ck}}}$.

4.1 Effect of longitudinal reinforcement ratio

Figure 6 presents the influence of longitudinal reinforcement ratio ρ_b on the normalized shear capacity $\lambda_n = V_n/(b_w h\sqrt{f_{ck}})$ of beams without web reinforcement for five different shear span

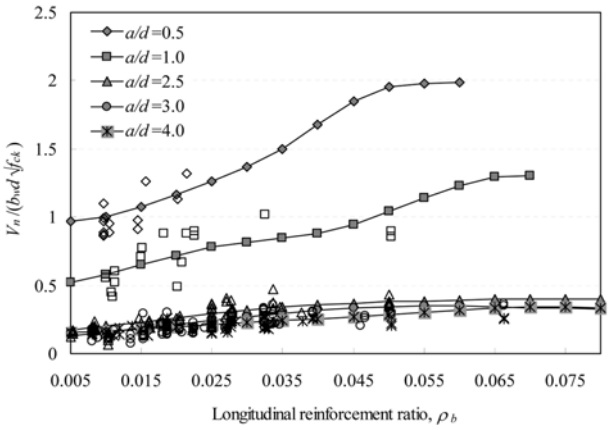

Fig. 6 Effect of ρ_b on normalized shear capacity of beams.

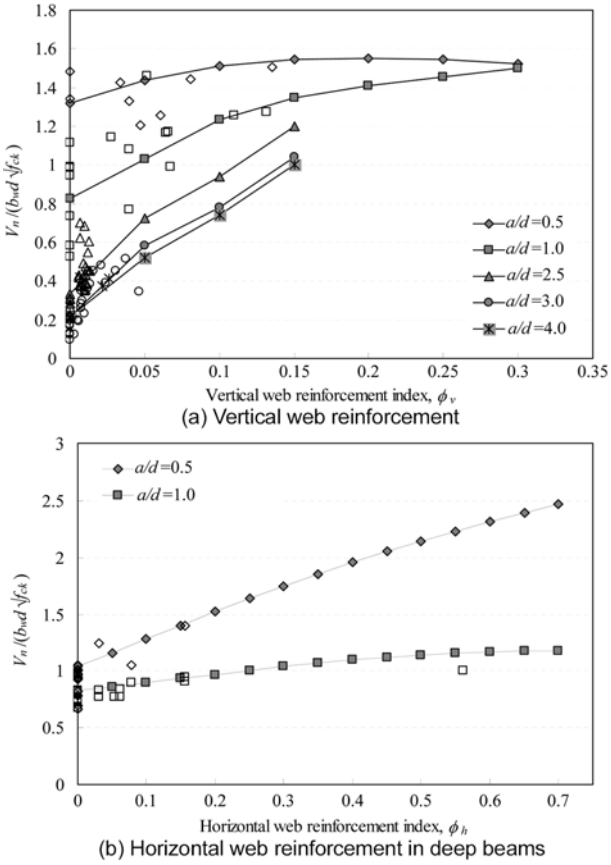

Fig. 7 Effect of web reinforcement on normalized shear capacity of beams.

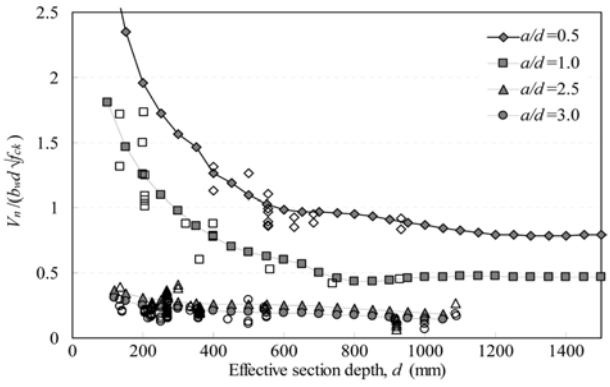

Fig. 8 Effect of d on normalized shear capacity of beams.

to depth ratios. The normalized shear capacity λ_n obtained from the developed NNs increases with the increase of ρ_b up to a certain limit beyond which λ_n remains constant, agreeing with test results. It is also observed that the influence of ρ_b on the λ_n is more notable in deep beams than slender beams.

4.2 Effect of web reinforcement

The influence of web reinforcement on λ_n of reinforced concrete beams is shown in Fig. 7; Fig. 7 (a) for vertical web reinforcement index ϕ_v and Fig. 7 (b) for horizontal web reinforcement index ϕ_h in deep beams. The vertical web reinforcement index ϕ_v has less effect on λ_n of deep beams having a/d of 0.5. On the other hand, the shear capacity of beams having a/d above 1.0 increases with the increase of ϕ_v. Therefore, it can be concluded that the effect of ϕ_v on the λ_n is nearly independent of a/d in slender beams, but significantly dependent on a/d in deep beams as proved by several researchers.[8,14,19] On the other hand, shear capacity of deep beams increases with the increase of ϕ_h, showing that a higher increasing rate develops in beams having a/d of 0.5 than in those with a/d of 1.0. This indicates that the smaller the a/d valve, the more effective the horizontal web reinforcement; however, the effectiveness of vertical web reinforcement is higher for larger a/d. From the deep beam tests, Tan et al[23]. also proposed that the critical shear span-to-overall depth ratio, where both vertical and horizontal web reinforcements are equally effective, is between 0.75 and 1.0.

4.3 Effect of effective section depth

The influence of effective section depth d on λ_n is presented in Fig. 8. Although, a slightly uneven trend occurred in the developed neural network for $a/d = 0.5$ because of the relatively small number of deep beams having $a/d = 0.5$ in the database, it is clearly observed that the normalized shear capacity λ_n of beams decreases with the increase of d; this is more notable in deep beams than slender beams as the transverse tensile strain in concrete struts increases with the decrease of a/d. However, no meaningful size effect appears in deep beams having d above 800 mm. It is also pointed out by Tan and Cheng[24] that the smaller a/d, the higher the size effect as it is greatly influenced by strut action carrying very high compressive forces as predicted by the trained NNs.

5. Conclusions

Optimum multi-layered feed-forward neural network (NN) models were built to predict the shear capacity of reinforced concrete slender and deep beams. The developed NNs used a resilient back-propagation algorithm and early stopping technique to improve training and generalization of neural network. In addition, an extensive database of 631 deep beams and 549 slender beams were established and then 50%, 25%, and 25% of all specimens in the database were selected for training, validation and test subsets, respectively. Based on the statistical comparisons and parametric analysis, the following conclusions may be drawn:

1) The predictions obtained from the developed NNs are in much better agreement with test results, regardless of the shear

span-to-depth ratio and amount of web reinforcement, than those determined from shear provisions of different codes, such as KBCS, ACI 318-05, and EC2. The mean and standard deviation of the ratio between predicted using the NNs and measured shear capacities are 1.02 and 0.18, respectively, for deep beams, and 1.04 and 0.17, respectively, for slender beams.

2) The influence of shear span-to-effective depth ratio on the shear capacity is more dominant in deep beams than slender beams. The shear capacity of beams having shear span-to-effective depth ratio more than 2.5 was little influenced by the variation of shear span-to-effective depth ratio.

3) The normalized shear capacity predicted from the neural network increases with the increase of longitudinal reinforcement ratio up to a certain limit beyond which it remains constant, agreeing with test results.

4) The effect of vertical web reinforcement on the normalized shear capacity is nearly independent of the shear span-to-effective depth ratio in slender beams, but significantly dependent of the shear span-to-effective depth ratio in deep beams. On the other hand, shear capacity of deep beams increases with the increase of the horizontal web reinforcement index, indicating that a higher increasing rate develops in beams having shear span-to-effective depth ratio of 0.5 than in those with shear span-to-depth ratio of 1.0.

5) The normalized shear capacity of beams decreases with the increase of effective depth of beam section, showing that the decreasing rate of shear capacity with the increase of the section depth is more notable in deep beams than slender beams.

Acknowledgments

This work was supported by the Regional Research Centers Program (Bio-housing Research Institute), granted by the Korean Ministry of Education & Human Resources Development. The authors wish to express their gratitude for the financial support.

Notation

A_h = area of horizontal web reinforcement
A_i = actual output of the data i
A_v = area of vertical web reinforcement
a = shear span
b_w = width of beam section
c = cover of longitudinal bottom reinfocement
d = effective depth of beam section
h = overall depth of beam section
f_{ck} = concrete compressive strength
f_y = yield strength of longitudinal reinforcement
f_{yh} = yield strength of horizontal web reinforcement
f_{yv} = yield strength of vertical web reinforcement
jd = distance between the center of top and bottom nodes
l_p = width of loading or support plate
p_i = original values of data set
$(p_i)_n$ = normalized values of data set
$(p_i)_{\max}$ = minimum value of the parameter under normalization
$(p_i)_{\min}$ = minimum value of the parameter under normalization
s_h = spacing of horizontal web reinforcement
s_v = spacing of vertical web reinforcement
T_i = target output of the data i
V_n = shear capacity of beams
w_s = width of concrete strut
w_t = depth of bottom node
w_t' = depth of top node
γ_{cs} = ratio of predicted and measured shear capacities
$\gamma_{cs,m}$ = average of γ_{cs}
$\gamma_{cs,s}$ = standard deviation of γ_{cs}
θ = angle of web reinforcement to longitudinal axis of beam
$(\theta_r)_j$ = angle between reinforcing bar j and the axis of cocrete strut
θ_s = angle between concrete strut and longitudinal axis of beam
λ_n = normalized shear strength $\left(\frac{V_n}{b_w d\sqrt{f_{ck}}}\right)$
ρ_h = horizontal web reinforcement ratio $\left(\frac{A_h}{b_w s_h}\right)$
ρ_b = longitudinal reinforcement ratio $\left(\frac{A_s}{b_w d}\right)$
ρ_v = vertical web reinforcement ratio $\left(\frac{A_v}{b_w s_v}\right)$
v_e = effectiveness factor of concrete
ϕ_b = longitudinal reinforcement index $\left(\frac{\rho_s f_y}{f_{ck}}\right)$
ϕ_h = horizontal web reinforcement index $\left(\frac{\rho_h f_{yh}}{f_{ck}}\right)$
ϕ_v = vertical web reinforcement index $\left(\frac{\rho_v f_{yv}}{f_{ck}}\right)$

References

1. MacGregor, J. G., *Reinforced Concrete: Mechanics and Design, Prentice-Hall International*, INC, 1997, 939pp.

2. ASCE-ACI Committee 445, "Recent Approaches to Shear Design of Structural Concrete," *Journal of Structural Engineering, ASCE*, Vol.124, No.12, 1998, pp.1375~1417.

3. Bohigas, A. C., S*hear Design of Reinforced High-Strength Concrete Beams*, Ph. D. Thesis, Technical University of Catalonia, 2002.

4. Collins, M. P., Mitchell, D., Adebar, P. E., and Vecchio, F. J., "A general Shear Design Method," *ACI Structural Journal*, Vol.93, No.1, 1996, pp.36~45.

5. Vecchio, F. J. and Collins, M. P., "The Modified Compression Field Theory for Reinforced Concrete Elements Subjected to Shear," *ACI Structural Journal*, Vol.83, No.2, 1986, pp.219~231.

6. Regan, P. E. "Research on Shear: a Benefit to Humanity or a Waste of Time?" *The Structural Engineer (London)*, Vol.71, No.19, 1993, pp.337~346.

7. Reineck, K. H., Kuchma, D. A., Kim, K. S., and Marx, S., "Shear Database for Reinforced Concrete Members without Shear Reinforcement," *ACI Structural Journal*, Vol.100, No.2, 2003, pp.240~249.

8. Yang, K. H. and Ashour, A. F., "Code Modelling of Rein-

forced Concrete Deep Beams," *Accepted for Publication in Magazine of Concrete Research*, 2007.

9. ACI Committee 318, *Building Code Requirements for Structural Concrete (318-99) and Commentary-(318R-99)*, American Concrete Institute, 1999.

10. *CIRIA Guide 2: The Design of Deep Beams in Reinforced Concrete*, Ove Arup and Partners, Construction Industry Research and Information Association, London, 1977.

11. ACI Committee 318, *Building Code Requirements for Structural Concrete (ACI 318-05) and Commentary (ACI 318R-05)*, American Concrete Institute, 2005.

12. The European Standard EN 1992-1-1:2004, *Eurocode 2: Design of concrete structures*, British Standards Institution, 2004.

13. Goh, A. T. C., "Prediction of Ultimate Shear Strength of Deep Beams Using Neural Networks," *ACI Structural Journal*, Vol.92, No.1, 1995, pp.28~32.

14. Sanad, A. and Saka, M. P., "Prediction of Ultimate Shear Strength of Reinforced-Concrete Deep Beams using Neural Networks," *Journal of Structural Engineering, ASCE*, Vol.127, No.7, 2001, pp.818~828.

15. Hagan, M. T. Demuth, H. B., and Beale, M. H., *Neural Network Design. Boston*, MA: PWS Publishing, 1996.

16. Architectural Institute of Korea, *Korean Building Code-Structural (KBCS)*, Kimoondang, 2005.

17. Shi, J. J., "Clustering Technique for Evaluating and Validating Neural Network Performance," *Journal of Computing in Civil Engineering, ASCE*, Vol.16, No.2 2002, pp.152~155.

18. Chung, J. C., *An Experimental Study on the Flexure-Shear Interaction Relation of RC Beams without Transverse Reinforcement*, MSc. Thesis, Chungang University in Korea, 2000.

19. Yang, K. H., Chung, H. S., and Ashour, A. F., "Influence of Shear Reinforcement on Reinforced Concrete Continuous Deep Beams," *Accepted for Publication in ACI Structural Journal*, 2007.

20. Demuth, H. and Beale, M., *Neural Network Toolbox for User with MATLAB*. The Math Works, Inc., USA, 2002.

21. Rumelhart, D. E., Hinton, G. E., and Williams, R. J., "Learning Representations by Back-propagation Error," *Nature*, Vol.323, 1986, pp.533~536.

22. Crist, R. A., "Shear Behavior of Deep Reinforced Concrete Beams," *Proceedings, Symposium on the Effects of Repeated Loading of Materials and Structural Elements*, Vol.4, RILEM, 1966, 31pp.

23. Tan, K. H., Kong, F. K., Teng, S., and Weng, L. W., "Effect of Web Reinforcement on High-Strength Concrete Deep Beams," *ACI Structural Journal*, Vol.94, No.5, 1997, pp.572~582.

24. Tan, K. H. and Cheng, G. H., "Size Effect on Shear Strength of Deep Beams: Investigating with Strut-and-Tie Model," *Journal of Structural Engineering, ASCE*, Vol.132, No.5, 2006, pp.673~685.